Neuro-Oncology

Neuro-Oncology 16(10), 1417–1426, 2014
doi:10.1093/neuonc/nou022
Advance Access date 5 March 2014

Accuracy of distinguishing between dysembryoplastic neuroepithelial tumors and other epileptogenic brain neoplasms with [^{11}C]methionine PET

Sylvain Rheims†, Sebastià Rubi†, Sandrine Bouvard, Emilien Bernard, Nathalie Streichenberger, Marc Guenot, Didier Le Bars, Alexander Hammers, and Philippe Ryvlin

Department of Functional Neurology and Epileptology and Institute of Epilepsies (IDEE) (S.Rh., E.B., P.R.); Department of Pathology (N.S.); Department of Functional Neurosurgery (M.G.); Hospices Civils de Lyon, Lyon, France; Lyon Neuroscience Research Center, INSERM U1028/CNRS UMR5292, Lyon, France (S.Rh., S.B., P.R.); CERMEP–Imagerie du Vivant, Lyon, France (S.B., D.L.B.); Neurodis Foundation, CERMEP–Imagerie du Vivant, Lyon, France (A.H.); Hospital Clinic de Barcelona, Barcelona, Spain (S.Ru.)

Corresponding Author: Philippe Ryvlin, MD, PhD, Department of Functional Neurology and Epileptology, Hospices Civils de Lyon, 59 boulevard Pinel, 69003 Lyon, France (ryvlin@cermep.fr).

†These authors contributed equally to this work.

Background. Dysembryoplastic neuroepithelial tumors (DNTs) represent a prevalent cause of epileptogenic brain tumors, the natural evolution of which is much more benign than that of most gliomas. Previous studies have suggested that [^{11}C]methionine positron emission tomography (MET-PET) could help to distinguish DNTs from other epileptogenic brain tumors, and hence optimize the management of patients. Here, we reassessed the diagnostic accuracy of MET-PET for the differentiation between DNT and other epileptogenic brain neoplasms in a larger population.

Methods. We conducted a retrospective study of 77 patients with focal epilepsy related to a nonrapidly progressing brain tumor on MRI who underwent MET-PET, including 52 with a definite histopathology. MET-PET data were assessed by a structured visual analysis that distinguished normal, moderately abnormal, and markedly abnormal tumor methionine uptake and by semiquantitative ratio measurements.

Results. Pathology showed 21 DNTs (40%), 10 gangliogliomas (19%), 19 low-grade gliomas (37%), and 2 high-grade gliomas (4%). MET-PET visual findings significantly differed among the various tumor types ($P < .001$), as confirmed by semiquantitative analyses ($P < .001$ for all calculated ratios), regardless of gadolinium enhancement on MRI. All gliomas and gangliogliomas were associated with moderately or markedly increased tumor methionine uptake, whereas 9/21 DNTs had normal methionine uptake. Receiver operating characteristics analysis of the semiquantitative ratios showed an optimal cutoff threshold that distinguished DNTs from other tumor types with 90% specificity and 89% sensitivity.

Conclusions. Normal MET-PET findings in patients with an epileptogenic nonrapidly progressing brain tumor are highly suggestive of DNT, whereas a markedly increased tumor methionine uptake makes this diagnosis unlikely.

Keywords: brain tumor, dysembryoplastic neuroepithelial tumor, epilepsy, methionine PET.

Brain tumors are among the most frequent causes of symptomatic focal epilepsy.[1] Although seizures can reveal aggressive neoplasms—such as high-grade gliomas and brain metastases—that require rapid oncologic management, epilepsy is frequently related to nonrapidly progressing brain tumors. Low-grade gliomas and glioneuronal tumors, such as gangliogliomas and dysembryoplastic neuroepithelial tumors (DNTs), are considered the most epileptogenic.[2]

From a clinical point of view, the discovery of a nonrapidly progressing lesion in a patient with epilepsy raises the question as to whether or not this lesion is at risk of malignant transformation and should be resected, regardless of seizure control. Malignant transformation is the rule in low-grade glial tumor and occurs in about 5% of gangliogliomas.[3] In contrast, DNTs are generally considered nonprogressive and not life threatening, with only

Received 25 April 2013; accepted 31 January 2014

very rare malignant transformations reported after brain radiotherapy.[4] Differentiation between DNT and other tumor types has thus a significant impact on patient management, in particular when the lesion is located in an eloquent area with significant risk of postoperative deficits. This issue is aggravated by the fact that biopsy is also likely to misdiagnose DNT if it is missing its specific glioneuronal component.[5]

Magnetic resonance imaging (MRI) may suggest the pathology underlying epileptogenic brain tumors,[6–9] with some features highly suggestive of DNT, including deformation of the overlying skull.[8,10] However, these features are lacking in a significant proportion of cases, especially in tumors with mesial temporal location. Accordingly, misclassifications have been repeatedly reported,[6,9] justifying the need to strengthen diagnosis with additional investigations.

[^{11}C]methionine PET (MET-PET) has been proposed as an additional tool to better grade nonrapidly progressing brain tumors.[11] High-grade gliomas are associated with higher methionine uptake than low-grade gliomas.[11] MET-PET has also been used to distinguish glioneuronal tumors from gliomas.[12–17] A previous study in our center[16] suggested that MET-PET might be a clinically useful and reliable predictor of the histopathology of epileptogenic brain tumors, with normal methionine uptake being suggestive of DNT. Although this previous study remains the largest MET-PET series of patients with nonrapidly progressing epileptogenic brain tumors, only 11 DNTs were included among the 27 participants.

Here, we review our center's experience with MET-PET for the differentiation between DNTs and other epileptogenic brain neoplasms in a total of 77 patients evaluated to date, including 52 with a definite histopathology.

Patients and Methods

We retrospectively reviewed the database of 131 patients who underwent MET-PET at our institution between January 1996 and December 2010.

Patients were selected according to the following criteria: (i) they underwent a MET-PET investigation for assessing an epileptogenic brain lesion compatible with a diagnosis of low-grade tumor, (ii) MRI was available for review, and (iii) MET-PET data were acquired on a high-resolution scanner (Siemens HR+), which quality enabled valid analysis. This selection process excluded: (i) 24 patients with epilepsy but no MRI lesion compatible with a diagnosis of brain tumor who underwent MET-PET as part of the specific ongoing protocol to characterize methionine uptake in nontumoral epileptogenic tissue, (ii) 4 patients with a noncortical mass-occupying lesion (including brainstem and spinal cord) and no epilepsy, (iii) 2 patients with a rapidly evolving brain tumor excluding the possibility of a low-grade tumor, (iv) 21 patients with a putative epileptogenic brain tumor without available MRI for review (referred from other institutions), and (v) 3 patients with major MET-PET artifacts that hampered any valid data analysis.

Among the remaining 77 patients, we then distinguished those for whom a reliable pathological diagnosis was available ($n = 52$) from those without such diagnosis, either because they were not operated on ($n = 19$) or because pathology remained inconclusive ($n = 6$). Only the 52 patients with a reliable pathology contributed to our primary analyses. Fifteen of them were previously reported by our group in a series that included 12 other patients scanned on a different low-resolution PET camera before 1996, not considered in the current study.[16]

MRI

MRI data were reviewed for all patients in order to specify tumor location and tumor size, as defined by the biggest diameter on axial T1 sequence, as well as the presence of bone deformation or gadolinium enhancement.

PET Data Acquisition

All patients underwent PET scanning using a high-resolution tomograph (HR+ Siemens), after an intravenous bolus injection of 18.5 ± 2.6 MBq/kg [^{11}C]methionine. Three-dimensional data were acquired and reconstructed into 63 slices, 2.4 mm thick, with an isotropic spatial resolution of ~5 mm full-width half-maximum. Before injection, transmission scanning for attenuation correction was carried out using 3 ^{68}Ge rod sources. Static emission scanning was performed during a 20-min period, beginning 35 min after [^{11}C]methionine injection, as previously proposed.[18–21] Images were corrected for scatter and attenuation and were reconstructed using a filtered backprojection.

PET Data Analysis

We conducted both visual and semiquantitative analyses of PET data, using similar methods to those previously described in detail.[16]

PET visual analysis was conducted by 2 investigators (S.Rh. and S.Ru.), blinded to all other clinical and MRI data except the anatomical location of the tumor. The visual analysis resulted in a classification based on the following definitions (Fig. 1):

Normal tumor methionine uptake: no visually detectable increased methionine uptake in the tumor compared with the surrounding or contralateral homotopic brain regions.

Moderately increased tumor methionine uptake: the tumor uptake clearly exceeds the uptake in surrounding cortical areas and in the contralateral homotopic region but remains lower or comparable to that of the contralateral occipital cortex that usually corresponds to the region of greatest methionine uptake.

Markedly increased tumor methionine uptake: the tumor uptake clearly exceeds the uptake in surrounding cortical areas as well as in the contralateral homotopic region and occipital cortex.

We performed a semiquantitative analysis using squared regions of interest (ROIs), 4.1 mm sided, directly placed onto the PET images. These ROIs were placed over the portion of the tumor displaying the highest [^{11}C]methionine uptake (T_s = tumor square ROI), the contralateral homotopic cortical region (C_s = contralateral square ROI), and the most active area within the contralateral occipital cortex (O_s = occipital square ROI), on a single slice each.[16] Two ratios were calculated:

Tumor to contralateral homotopic ratio (TC_r) = T_s/C_s.
Tumor to contralateral occipital ratio (TO_r) = T_s/O_s.

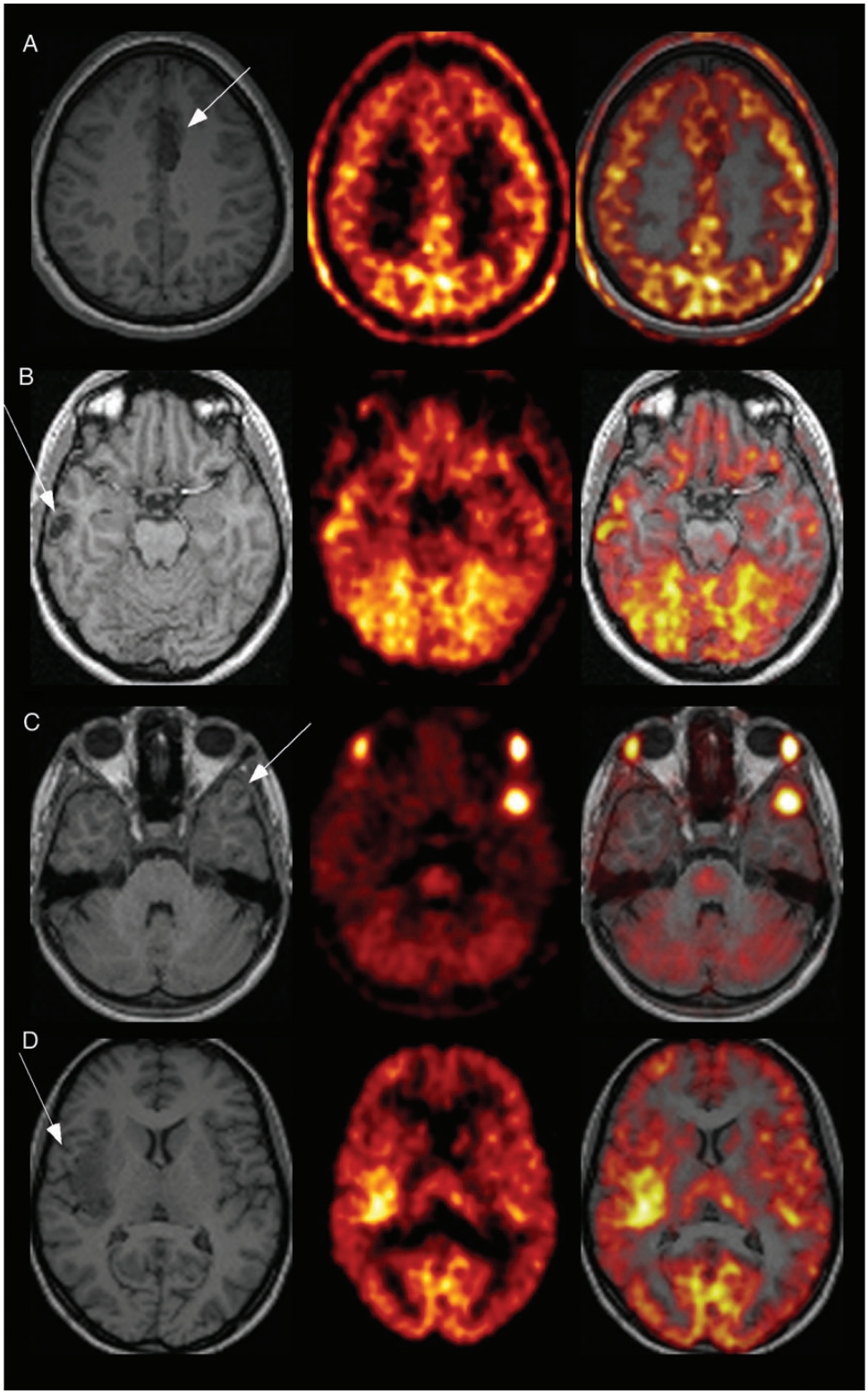

Fig. 1. Examples of T1-weighted MRIs (left panel), methionine uptake on MET-PET (middle panel), and coregistered MRI and PET data (right panel) for the 3 major tumor types. (A) Left mesial frontal DNT, which was not associated with a visually detectable increased methionine uptake (patient #9). (B) Right neocortical (temporal) DNT observed on T1-weighted MRI with a moderately increased methionine uptake (patient #6). (C) Left temporal ganglioglioma associated with a markedly increased methionine uptake (patient #30). (D) Right insular low-grade glioma associated with a moderately increased methionine uptake (patient #34).

Surgical Procedure and Pathological Data

Thirty-two patients (55%) had a total removal and 26 (45%) a subtotal removal of their tumor. Sections of formalin-fixed tissue were processed for histological staining using either the hemalum-phloxine-safranin or the hematoxylin-eosin technique. Immunohistochemical stains, applied on routinely fixed and paraffin-embedded sections, were prepared for selected cases, using the avidin–biotin complex method and the following antisera: anti–glial fibrillary acidic protein, anti–neurofilament protein, anti–neurone-specific enolase, antisynaptophysin, anti-vimentin, anti–S100 protein, and anti–Leu-7. A Ki-67 labeling index was obtained in 29 patients.

All specimens but one (#13) were analyzed at our institution by neuropathologists trained in the evaluation of epileptogenic low-grade tumors and were ultimately classified according to World Health Organization grade. The specimens of 15 patients were sent to 2 other pathologists renowned for their experience in epileptogenic brain tumors (C. Daumas-Duport, Saint-Anne Hospital, Paris, and B. Pasquier, Albert Michallon Hospital, Grenoble, France) for further evaluation. Pathology remained inconclusive in 6 of the 58 patients operated on.

Statistical Analysis

For both visual and semiquantitative analyses, 4 types of tumor were considered: DNTs, gangliogliomas, low-grade gliomas, and high-grade gliomas. We searched for tumor correlations among type, anatomical location, and size, as well as the presence of contrast enhancement on MRI and that of a visually detectable increased tumor methionine uptake on MET-PET images, using the Fisher exact probability test and the Mann–Whitney test, with level of significance at $P < .05$. For the semiquantitative MET-PET analysis, we used the Kruskal–Wallis test. We looked at correlations between semiquantitative analysis and visual analysis using linear regression. Receiving operating characteristics (ROC) curves were generated and area under the curves (AUCs) were determined. Comparison of curves was performed using MedCalc 12.4.

Results

Data From the 52 Patients With a Definite Pathological Diagnosis

Clinical and pathological data

There were 27 men and 25 women with a mean ± SD age at epilepsy onset of 25 ± 16 years and mean ± SD duration of epilepsy of 7 ± 8 years (range, 3 mo–39 y) (Table 1). Pathological examination revealed a DNT in 21 patients (40.5%), including 2 with a pilocytic component (#23, #39), 1 of whom also had associated focal cortical dysplasia (#23). Twenty-one patients (40.5%) had a glioma, including 14 oligodendrogliomas (12 grade II and 2 grade III), 5 grade II oligoastrocytomas, and 2 grade II astrocytomas, and the remaining 10 patients (19%) had a ganglioglioma.

MRI findings

Thirty-three tumors (63%) were located in the temporal lobe, including 17 (33%) within the mesial temporal structures. Nineteen tumors (37%) were located in the frontal lobe, 7 in the insula (14%), 5 in the parietal lobe (10%), and 4 in the occipital lobe (8%) (Table 2). Tumor location significantly varied across tumor types ($P < .001$), with a mesial temporal location more frequent for DNTs (57%) than for gangliogliomas (40%) and gliomas (5%). Mean tumor size was significantly larger for low-grade gliomas (49 ± 18 mm) than for DNTs (26.4 ± 11.3 mm) and gangliogliomas (20.1 ± 13.6 mm) ($P < .001$). Bone deformation was observed in 3 DNTs (14%). T1-weighted imaging after the administration of gadolinium contrast material was available in 48 patients (92%). Gadolinium enhancement was more frequently observed in gangliogliomas (75%) than in other tumor types (10% of DNTs, 17% of low-grade gliomas, and 50% of high-grade gliomas, $P = .002$).

MET-PET findings

Visual analysis demonstrated an increased methionine uptake within the tumor in 43 patients (83%), which was classified as markedly so in 20 (39%) and moderately so in 23 (44%). In 9 patients (17%), no increased uptake was detected.

Methionine uptake was not correlated with tumor size or tumor location (Table 3). There was no significant association between visual methionine uptake and gadolinium enhancement on MRI ($P = .124$), even though an increased methionine uptake (moderate or marked) was detected in all patients with gadolinium enhancement. Indeed, increased methionine uptake was also observed in 75% of those without gadolinium enhancement.

MET-PET findings on visual analysis correlated with pathological data ($P < .001$; Table 4). Normal methionine uptake was observed in only DNTs, where it was noted in 9/21 (43%) patients. Markedly increased methionine uptake was observed in 2/2 (100%) high-grade gliomas, 6/10 (60%) gangliogliomas, 10/19 (53%) low-grade gliomas, and only 2/21 (10%) DNTs. Interestingly, these 2 DNTs were those associated with a pilocytic component (patients #23 and #39). Moderately increased methionine uptake was observed in 10/21 (48%) DNTs, 9/19 (47%) low-grade gliomas, and 4/10 (40%) gangliogliomas. These results remained similar in the subset of mesial temporal lesions, where 5/12 (42%) DNTs demonstrated normal uptake. There was no significant correlation between methionine uptake and Ki-67 index.

Mean values of TC_r and TO_r for each tumor type are given in Table 5. Both ratios significantly differed across tumor types ($P < .001$ for TC_r and $P < .001$ for TO_r). Post-hoc analyses showed that DNTs were associated with lower ratios than gangliogliomas (TC_r: $P = .001$; TO_r: $P < .001$), low-grade gliomas (TC_r: $P = .005$; TO_r: $P < .001$), and high-grade gliomas (TC_r: $P = .022$; TO_r: $P = .022$). In addition, there was a trend toward lower uptake values in gangliogliomas than in high-grade gliomas (TC_r: $P = .086$; TO_r: $P = .053$). In contrast, low-grade gliomas did not differ from gangliogliomas or from high-grade gliomas. Semiquantitative analyses correlated with the results of visual analyses ($r = 0.751$ and $P < .001$ for TC_r and $r = 0.767$ and $P < .001$ for TO_r; see Supplementary Fig. 1).

ROC curves were plotted to assess the sensitivity and specificity of TC_r and TO_r to discriminate DNTs from other tumor types (Fig. 2). Estimates of AUCs were 0.88 (95% confidence interval [CI]: 0.76–0.95) for TC_r and 0.95 (95% CI: 0.85–0.99) for TO_r, implying significant discriminatory power of both markers in this patient population ($P < .0001$ for AUC > 0.5, DeLong test). As shown

Table 1. Individual pathological, clinical, MRI, and MET-PET data from the 52 patients with definite pathology

Clinical Data					MRI Data				MET-PET Data			Pathology
Patient No.	Gender	Age, y	Epilepsy Onset, y	Epilepsy Duration, y	Location	Side	Tumor Size (biggest diameter, mm)	Gd	Uptake on Visual Analysis	TC_r	TO_r	
1	F	21	3	18	mT + O	L	55	−	Normal	0.89	0.60	DNT
3	M	64	54	10	mT	R	18	−	Normal	1.11	0.84	DNT
6	F	39	38	1	lT	R	20	−	Moderate	1.25	0.92	DNT
7	F	42	37	5	mT	R	19	−	Normal	0.55	0.38	DNT
9	F	17	6	11	Fr	L	30	−	Normal	0.92	0.67	DNT
11	M	5	4	1	Fr	L	16	−	Normal	0.93	0.74	DNT
12	F	27	25	1.5	lT	L	27	NA	Moderate	1.81	1.11	DNT
17	M	37	34	3	mT	L	10	+	Moderate	1.44	0.81	DNT
21	M	15	14	1	Fr + I	L	37	−	Normal	0.90	0.88	DNT
22	F	48	39	9	mT	L	20	−	Moderate	1.63	1.02	DNT
24	M	12	9	3	lT	L	39	−	Normal	0.91	0.57	DNT
26	F	46	38	8	Fr + P	R	48	−	Moderate	1.35	0.93	DNT
28	F	18	8	10	mT + lT	L	29	−	Moderate	1.46	0.95	DNT
32	F	12	11	1	lT	R	15	−	Moderate	1.70	1.09	DNT
40	M	32	18	14	mT	L	25	−	Normal	0.71	0.52	DNT
43	F	10	7	3	lT + O	L	36	−	Moderate	1.49	1.00	DNT
47	M	27	18	9	mT	L	23	−	Moderate	1.44	0.88	DNT
49	F	18	17	1	mT	L	17	−	Moderate	1.44	0.94	DNT
50	F	62	55	7	mT	R	20	−	Normal	1.38	0.82	DNT
23	M	51	21	30	mT	R	30	+	Marked	2.29	1.44	DNT + pilocytic component
39	F	39	35	4	mT	R	21	−	Marked	1.86	1.21	DNT + pilocytic component
2	F	35	18	17	lT + I + Fr	L	56	+	Marked	2.21	1.63	Ganglioglioma
4	M	6	5	1	mT	L	15	NA	Marked	2.46	1.53	Ganglioglioma
5	M	12	10	2	mT	R	22	+	Moderate	1.93	1.11	Ganglioglioma
19	M	19	11	8	lT	R	10	+	Marked	2.06	1.61	Ganglioglioma
29	F	33	30	3	mT	R	15	−	Moderate	1.42	0.93	Ganglioglioma
30	F	13	8	5	lT	L	14	−	Marked	2.90	2.03	Ganglioglioma
33	M	15	9	6	lT	R	16	+	Marked	1.78	1.45	Ganglioglioma
37	M	45	20	25	lT	L	15	NA	Marked	2.07	1.43	Ganglioglioma
45	F	43	4	39	lT + P	R	28	+	Moderate	1.59	1.13	Ganglioglioma
46	F	16	2	14	mT	L	21	+	Moderate	2.16	1.29	Ganglioglioma
8	F	37	34	3	mT + O	L	90	−	Marked	2.58	2.14	Oligoastrocytoma II
10	M	20	19	1	Fr	L	53	−	Marked	1.76	1.29	Oligodendroglioma II
13	M	28	27	1	Fr	R	30	−	Moderate	1.53	1.09	Oligoastrocytoma II
14	F	64	63.5	0.5	Fr	R	28	−	Marked	2.17	1.51	Oligodendroglioma II
16	M	38	37.5	0.5	Fr	R	36	−	Moderate	1.46	1.14	Oligodendroglioma II
18	M	41	35	6	P + lT	L	52	−	Marked	2.89	2.04	Oligodendroglioma II
20	M	42	33	9	Fr	R	26	−	Moderate	1.50	1.15	Oligoastrocytoma II
27	F	39	38	1	lT + I	R	60	−	Marked	5.35	3.41	Astrocytoma II
31	M	40	37	3	lT	L	69	−	Marked	2.44	1.71	Astrocytoma II
34	F	24	16	8	I	R	54	−	Moderate	1.31	1.07	Oligoastrocytoma II
35	M	26	25	0.66	Fr + I	R	69	−	Marked	2.34	1.32	Oligoastrocytoma II
36	F	53	46	7	lT + I	L	45	+	Moderate	1.28	0.93	Oligodendroglioma II
38	M	40	25	15	Fr	L	33	−	Marked	2.42	1.69	Oligodendroglioma II
41	M	37	36	1	Fr	R	35	−	Marked	2.94	1.74	Oligodendroglioma II
42	M	28	27	1	Fr	R	20	+	Moderate	1.33	1.05	Oligodendroglioma II
44	M	38	37	1	Fr + P	L	60	NA	Moderate	1.24	1.23	Oligodendroglioma II
48	F	7	0	7	lT + I + Fr	L	62	−	Moderate	1.46	0.87	Oligodendroglioma II

Continued

Table 1. *Continued*

Clinical Data					MRI Data				MET-PET Data			Pathology
Patient No.	Gender	Age, y	Epilepsy Onset, y	Epilepsy Duration, y	Location	Side	Tumor Size (biggest diameter, mm)	Gd	Uptake on Visual Analysis	TC_r	TO_r	
51	M	49	47	2	Fr	L	60	+	Moderate	1.48	1.10	Oligodendroglioma II
52	M	48	49	0.3	Fr	L	54	−	Marked	1.63	1.09	Oligodendroglioma II
15	F	50	44	6	P + O	L	43	−	Marked	2.58	1.67	Oligodendroglioma III
25	M	49	18	31	Fr	L	40	+	Marked	2.65	2.11	Oligodendroglioma III

Abbreviations: Gd, gadolinium; DNT, dysembryoplastic neuroepithelial tumors.

Table 2. Correlation between pathology and MRI data

MRI Data	Pathological Data				Total	*P**
	DNT	Gangliogliomas	Low-grade Gliomas	High-grade Gliomas		
Total	21	10	19	2	52	−
Tumor size, mm (mean ± SD)	26.4 (11.3)	20.1 (13.6)	49.2 (18.1)	41.5 (2.1)	34.1 (18.6)	<.001
Location, *n* (%)						
Mesial Temporal lobe	12 (57)	4 (40)	1 (5)	0	17 (33)	<.001
Other	9 (43)	6 (60)	18 (95)	2 (100)	35 (67)	
Bone deformation,*n* (%)	3 (14)	0	0	0	3 (6)	.304
Gadolinium enhancement, *n* (%)						
+	2 (10)	6 (75)	3 (17)	1 (50)	12 (25)	.002
−	18 (90)	2 (25)	15 (83)	1 (50)	36 (75)	

*Fisher exact probability test or the Mann–Whitney test.

Table 3. Correlation between qualitative MET-PET data and MRI data

MRI Data	Visual Methionine Uptake			Total	*P**
	Normal	Moderate Increase	Marked Increase		
Total	9	23	20	52	−
Tumor size, mm (mean ± SD)	28.8 (12.9)	31 (16.3)	40.1 (22.2)	34.1 (18.6)	.404
Location, *n* (%)					
Mesial Temporal lobe	5 (55)	8 (35)	4 (20)	17 (33)	.157
Other	4 (45)	15 (65)	16 (80)	35 (67)	
Bone deformation, *n* (%)	1	2	0	3 (6)	.386
Gadolinium enhancement, *n* (%)					
+	0	7 (33)	5 (28)	12 (25)	.124
−	9 (100)	14 (67)	13 (72)	36 (75)	

*Fisher exact probability test or the Mann–Whitney test.

in Table 6, $TC_r < 1.31$ or $TO_r < 1.02$ predicted DNT with 90% specificity and with 47% and 89% sensitivity, respectively. Comparison of AUCs for TC_r and TO_r showed slight but statistically significant superiority of TO_r over TC_r ($P = .02$, DeLong test). To quantitatively assess the potential added diagnostic power of combining TC_r and TO_r results in this study population, we performed a logistic regression analysis with TC_r and TO_r as independent variables and diagnosis of DNT as the dependent variable. In this bivariate analysis, diagnosis of DNT was associated with TO_r ($P = .006$) but not with TC_r ($P = .132$), suggesting that the combination of these markers did not increase the probability of DNT diagnosis. As a matter of fact, comparison of ROC curves for TC_r, TO_r, and their joint regression-derived bivariate marker showed that the AUC for the bivariate marker (0.92 [95%

Table 4. Correlation between qualitative MET-PET data and pathology ($P < .001$)

Pathological Data	Visual Methionine Uptake, *n* (%)			Total
	Normal	Moderate Increase	Marked Increase	
DNT	9 (43)	10 (48)	2 (9)	21
Ganglioglioma	0	4 (40)	6 (60)	10
Low-grade gliomas	0	9 (47)	10 (53)	19
High-grade gliomas	0	0	2 (100)	2

Table 5. Correlation between semiquantitative MET-PET and pathological data

Pathological Data	*n* Patients	TC_r, mean (95% CI)	TO_r, mean (95% CI)
DNT	21	1.31 (1.11–1.50)	0.87 (0.76–0.98)
Ganglioglioma	10	2.06 (1.75–2.36)	1.41 (1.19–1.64)
Low-grade gliomas	19	2.06 (1.59–2.53)	1.45 (1.16–1.74)
High-grade gliomas	2	2.61 (2.18–3.05)	1.89 (0–4.7)

$P < .001$ for both TC_r and TO_r.

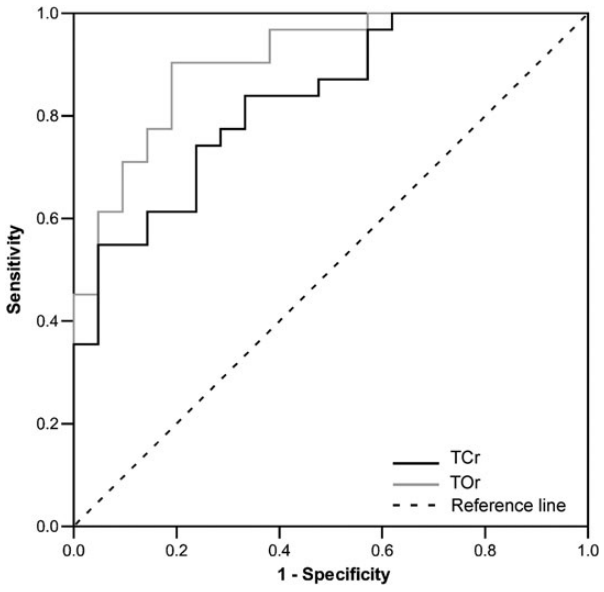

Fig. 2. ROC curves for TC_r and TO_r when used to discriminate DNTs from other tumor types. Blue line indicates ROC curve for TC_r; green line indicates ROC curve for TO_r; dotted line indicates diagonal representing a hypothetical test with no diagnostic discrimination.

CI: 0.81–0.98]) differed neither from the AUC for TC_r ($P = .053$, DeLong test) nor from the AUC for TO_r ($P = .568$, DeLong test).

To evaluate whether the diagnostic contribution of MET-PET remained clinically pertinent after the integration of MRI data, we performed a logistic regression analysis with diagnosis of DNT as the dependent variable and with TO_r and MRI findings as independent variables. In this multivariate analysis, diagnosis of DNT was associated with TO_r ($P = .03$) but not with tumor size ($P = .250$), observation of gadolinium enhancement ($P = .166$), bone deformation ($P = .99$), or mesial temporal location ($P = .154$).

Data From the 25 Patients Without a Definite Pathological Diagnosis

There were 11 men and 14 women with a mean ± SD age at epilepsy onset of 21 ± 13 years and mean ± SD duration of epilepsy of 14 ± 14 years (range, 1 mo–46 y) (Supplementary Table 1). As detailed in Supplementary Table 2, visual analysis demonstrated no increased methionine uptake within the tumor in 9 patients (36%), a moderately increased uptake in 8 (32%), and a markedly increased uptake in 8 (32%). Mean values of TC_r and TO_r were 1.54 (95% CI: 1.24–1.84) and 1.06 (95% CI: 0.87–1.25), respectively. Twelve patients (48%), including 10 among those who had not been operated on, showed TO_r suggestive of DNT (ie, $TO_r < 1.02$). MRI follow-up was available in 15 patients (60%, mean ± SD follow-up of 5.4 ± 2.2 y), including 8 of the 9 with normal methionine uptake and $TO_r < 1.02$ (mean ± SD follow-up of 6.2 ± 2.2 y). Only 1 of these 15 patients (#55), in whom MET-PET showed marked methionine uptake, demonstrated tumor progression on MRI suggestive of underlying low-grade glioma.

Discussion

In comparison with previous published series,[12–17] the present work provides significant updates about the diagnostic accuracy of MET-PET for the differentiation of DNTs from other tumor types in patients with nonrapidly progressing epileptogenic brain tumors: (i) normal methionine uptake was observed in only DNTs; (ii) DNTs are rarely associated with a markedly increased methionine uptake, which, when observed, appears to reflect the presence of a pilocytic component; (iii) the TO_r obtained from the semiquantitative analysis of methionine uptake distinguished DNT from other tumor types with 89% sensitivity and 90% specificity; and (iv) gangliogliomas and gliomas were always associated with an increased methionine uptake, which could be marked or moderate, without a distinctive MET-PET feature between these 2 tumor types.

Several authors have emphasized the difficulties in establishing the neuropathological diagnosis of DNT.[5,22] The diagnosis is partly based on the presence of specific glioneuronal components with "floating neurons," a specific histological feature that could be missing in nonspecific forms of DNT[5,23] or when the tumor has been removed incompletely. This could represent a limitation in the interpretation of our data, especially for patients with incomplete resection. However, this risk was minimized by our stringent reliability criteria for pathological diagnosis, including ability to obtain reevaluation by experts in the field of glioneuronal tumors whenever necessary.

One of the main results of our study is that in the presence of MRI findings suggesting a nonrapidly progressing brain tumor, normal MET-PET was observed in only DNTs, whereas gangliogliomas and gliomas always led to an increase in methionine uptake. This result is in line with our previous report[16] and is consolidated

Table 6. Performance characteristics of TC_r and TO_r to discriminate DNT from other tumor types

Semiquantitatively Derived Ratios	Threshold	Sensitivity		Specificity	
		%	95% CI	%	95% CI
TC_r	≤1.1069	42.11	20.3–66.5	100	89.4–100
	≤1.3752	57.89	33.5–79.7	87.88	71.8–96.6
	≤1.4605	78.95	54.4–93.9	78.79	61.1–91.0
TO_r	≤0.8362	47.37	24.4–71.1	100	89.4–100
	≤1.0193	89.47	66.9–98.7	90.91	75.7–98.1
	≤1.112	100	82.4–100	72.73	54.5–86.7

by the larger sample size of the current study. When data from the 2 series are pooled together (ie, including 12 more patients scanned on a low-resolution PET camera[16]), a total of 13 patients showed normal methionine uptake, and all had DNTs. However, the lack of pathological diagnosis in one-third of our cohort of patients with a suspected epileptogenic brain tumor and available MRI and MET-PET data questions the external validity of our findings. One might speculate that reassuring MET-PET findings have influenced the decision not to operate on some of these patients, an hypothesis consistent with the twice greater rate of tumors without increased methionine uptake in patients not operated on than in those operated on (40% vs 19%). This selection bias carries the risk that a non-DNT associated with normal methionine uptake could have been missed. However, follow-up data from patients not operated on who had normal methionine uptake failed to identify any sign of MRI progression over a mean of 6.2 years. Some authors have reported the possibility of normal MET-PET findings in low-grade gliomas.[18,24–26] It should be noted that some of these studies were conducted before DNT was clearly recognized, suggesting the possibility that some of these astrocytomas would be classified as DNTs today.[24,26]

Interestingly, the only 2 DNTs with markedly increased methionine uptake showed a specific histological pattern, including a pilocytic component. It has been reported that methionine uptake is increased in pilocytic astrocytoma, with values that can be higher than in grade II astrocytoma.[13] It might thus be speculated that the unusual MET-PET pattern observed in these 2 DNTs was primarily related to the presence of a pilocytic component.

Unlike normal MET-PET findings, the various degrees of increased visual methionine uptake did not discriminate among the different tumors. However, semiquantitative analyses provided complementary information that could help increase the diagnostic accuracy of MET-PET. Indeed, the 2 ratios obtained from the semiquantitative analyses, TC_r and TO_r, showed significant discriminatory power between DNTs and other tumor types, though TC_r showed lower sensitivity than TO_r. Specifically, a cutoff threshold of 1.02 for TO_r distinguished DNTs from other tumor types with 89% sensitivity and 90% specificity. The lower sensitivity of TC_r might have been related to greater interindividual variability of the methionine uptake within the contralateral homotopic nontumoral cortex than within the occipital cortex, which spontaneously demonstrate high methionine uptake.

Other radiolabeled amino acids, including [^{18}F]fluoroethyl-L-tyrosine and alpha-[^{11}C]methyl-L-tryptophan, have been proposed for the PET diagnosis of nonrapidly progressing brain tumors but failed to discriminate among the different gliomas and glioneuronal tumors, including DNTs.[27,28]

A prevailing hypothesis is that the increased methionine uptake observed in tumoral cells reflects an upregulation of the amino acid transport system[29–31] caused by increased protein metabolism and cellular proliferation.[31,32] It has also been suggested that the breakdown of the blood–brain barrier, as partly reflected by the presence of gadolinium enhancement on MRI, significantly contributes to MET-PET abnormalities.[33] Our results were only partly consistent with these hypotheses. While DNTs, which are characterized by a low proliferative index,[5,34] demonstrated lower methionine uptake than low-grade gliomas, this was not the case for gangliogliomas, even though these glioneuronal tumors are also characterized by low proliferative index.[35,36] Furthermore, we failed to find correlation between methionine uptake and the proliferative index Ki-67. Although all tumors associated with gadolinium enhancement on MRI showed increased methionine uptake, blood–brain barrier disruption was not associated with the intensity of MET-PET abnormalities. Indeed, gadolinium enhancement was observed in 33% of tumors with moderately increased methionine uptake versus 25% of those with a markedly increased uptake. Epileptic activity might contribute to the abnormal metabolism of amino acids. Indeed, methionine uptake was found increased in nontumoral epileptic lesions, such as focal cortical dysplasia.[37,38] Since the intrinsic epileptic activity of DNTs and gangliogliomas appears greater than that of low-grade gliomas,[2] possibly due to the presence of neuronal cells, one might hypothesize that this putative mechanism of methionine uptake could play a greater role in glioneuronal tumors compared with gliomas. Overall, the level of methionine uptake within nonrapidly progressing epileptogenic tumors might reflect a combination of cellular proliferation (greater in gliomas), blood–brain barrier disruption (more frequent in gangliogliomas and high-grade gliomas), intrinsic epileptic activity (greater in DNTs and gangliogliomas), and other, yet unknown factors, accounting for the overlapping MET-PET patterns observed among all tumor types.

From a clinical point of view, the preoperative distinction of DNT from other epileptogenic tumors has important consequences. One of the main issues in patients with brain tumor and long-standing partial epilepsy is to evaluate whether there is an oncological indication for surgery. Thus, the risk of malignant transformation is usually prioritized over surgical risks, including postoperative neuropsychological deficits when the tumor is located within language or memory networks. In contrast, surgery is usually forgone for benign tumors located within an

eloquent cortex. As a rule, DNTs are benign, with rare recurrences and a single published case of suspected spontaneous malignant transformation.[4,39] However, MRI cannot predict the histological diagnosis of DNT with certainty, especially in tumors with mesial temporal location.[6,9] In that perspective, normal MET-PET finding might be of particular importance in the decision process. Thus, the correlation between normal methionine uptake and a pathological diagnosis of DNT might be strong enough to allow deferring decision of tumor surgical removal when MET-PET is normal both in seizure-free patients and in patients with tumor located within eloquent cortex, including tumors located within the left mesial temporal structures in right-handed patients.

Supplementary Material

Supplementary material is available online at *Neuro-Oncology* (http://neuro-oncology.oxfordjournals.org/).

Funding

S.Ru. was supported by the Fundació Universitària Agustí Pedro i Pons, Universitat de Barcelona.

Acknowledgments

We wish to thank Professors C. Daumas-Duport, Saint-Anne Hospital, and B. Pasquier, Albert Michallon Hospital, for reviewing some of the pathological specimens.

We also thank Drs Hélène Catenoix, Genevieve Demarquay, Catherine Fischer, Jean Isnard, Dominique Rosenberg, and Pr François Mauguière for help in recruitment of patients.

Conflict of interest statement. None declared.

References

1. Olafsson E, Ludvigsson P, Gudmundsson G, et al. Incidence of unprovoked seizures and epilepsy in Iceland and assessment of the epilepsy syndrome classification: a prospective study. *Lancet Neurol*. 2005;4(10):627–634.
2. Ruda R, Trevisan E, Soffietti R. Epilepsy and brain tumors. *Curr Opin Oncol*. 2010;22(6):611–620.
3. DeMarchi R, Abu-Abed S, Munoz D, et al. Malignant ganglioglioma: case report and review of literature. *J Neurooncol*. 2011;101(2):311–318.
4. Ray WZ, Blackburn SL, Casavilca-Zambrano S, et al. Clinicopathologic features of recurrent dysembryoplastic neuroepithelial tumor and rare malignant transformation: a report of 5 cases and review of the literature. *J Neurooncol*. 2009;94(2):283–292.
5. Daumas-Duport C. Dysembryoplastic neuroepithelial tumours. *Brain Pathol*. 1993;3(3):283–295.
6. Campos AR, Clusmann H, von Lehe M, et al. Simple and complex dysembryoplastic neuroepithelial tumors (DNT) variants: clinical profile, MRI, and histopathology. *Neuroradiology*. 2009;51(7):433–443.
7. Cavaliere R, Lopes MB, Schiff D. Low-grade gliomas: an update on pathology and therapy. *Lancet Neurol*. 2005;4(11):760–770.
8. Chassoux F, Rodrigo S, Mellerio C, et al. Dysembryoplastic neuroepithelial tumors: an MRI-based scheme for epilepsy surgery. *Neurology*. 2012;79(16):1699–1707.
9. Stanescu Cosson R, Varlet P, Beuvon F, et al. Dysembryoplastic neuroepithelial tumors: CT, MR findings and imaging follow-up: a study of 53 cases. *J Neuroradiol*. 2001;28(4):230–240.
10. Daumas-Duport C, Varlet P, Bacha S, et al. Dysembryoplastic neuroepithelial tumors: nonspecific histological forms—a study of 40 cases. *J Neurooncol*. 1999;41(3):267–280.
11. Petrirena GJ, Goldman S, Delattre JY. Advances in PET imaging of brain tumors: a referring physician's perspective. *Curr Opin Oncol*. 2011;23(6):617–623.
12. Braun V, Dempf S, Weller R, et al. Cranial neuronavigation with direct integration of (11)C methionine positron emission tomography (PET) data—results of a pilot study in 32 surgical cases. *Acta Neurochir (Wien)*. 2002;144(8):777–782; discussion 782.
13. Galldiks N, Kracht LW, Berthold F, et al. [11C]-L-methionine positron emission tomography in the management of children and young adults with brain tumors. *J Neurooncol*. 2010;96(2):231–239.
14. Kaplan AM, Lawson MA, Spataro J, et al. Positron emission tomography using [18F] fluorodeoxyglucose and [11C] l-methionine to metabolically characterize dysembryoplastic neuroepithelial tumors. *J Child Neurol*. 1999;14(10):673–677.
15. Maehara T, Nariai T, Arai N, et al. Usefulness of [11C]methionine PET in the diagnosis of dysembryoplastic neuroepithelial tumor with temporal lobe epilepsy. *Epilepsia*. 2004;45(1):41–45.
16. Rosenberg DS, Demarquay G, Jouvet A, et al. [11C]-methionine PET: dysembryoplastic neuroepithelial tumours compared with other epileptogenic brain neoplasms. *J Neurol Neurosurg Psychiatry*. 2005;76(12):1686–1692.
17. Torii K, Tsuyuguchi N, Kawabe J, et al. Correlation of amino-acid uptake using methionine PET and histological classifications in various gliomas. *Ann Nucl Med*. 2005;19(8):677–683.
18. De Witte O, Goldberg I, Wikler D, et al. Positron emission tomography with injection of methionine as a prognostic factor in glioma. *J Neurosurg*. 2001;95(5):746–750.
19. Herholz K, Holzer T, Bauer B, et al. 11C-methionine PET for differential diagnosis of low-grade gliomas. *Neurology*. 1998;50(5):1316–1322.
20. Kincaid PK, El-Saden SM, Park SH, et al. Cerebral gangliogliomas: preoperative grading using FDG-PET and 201Tl-SPECT. *AJNR Am J Neuroradiol*. 1998;19(5):801–806.
21. Roelcke U, Radu EW, Hausmann O, et al. Tracer transport and metabolism in a patient with juvenile pilocytic astrocytoma. A PET study. *J Neurooncol*. 1998;36(3):279–283.
22. Pasquier B, Peoc'H M, Fabre-Bocquentin B, et al. Surgical pathology of drug-resistant partial epilepsy. A 10-year-experience with a series of 327 consecutive resections. *Epileptic Disord*. 2002;4(2):99–119.
23. Varlet P, Beuvon F, Fallet-Bianco C, et al. [Dysembryoplastic neuroepithelial tumors]. *Ann Pathol*. 2000;20(5):429–437.
24. Bustany P, Chatel M, Derlon JM, et al. Brain tumor protein synthesis and histological grades: a study by positron emission tomography (PET) with C11-L-methionine. *J Neurooncol*. 1986;3(4):397–404.
25. Derlon JM, Petit-Taboue MC, Chapon F, et al. The in vivo metabolic pattern of low-grade brain gliomas: a positron emission tomographic study using 18F-fluorodeoxyglucose and 11C-L-methylmethionine. *Neurosurgery*. 1997;40(2):276–287; discussion 287–288.
26. Ogawa T, Shishido F, Kanno I, et al. Cerebral glioma: evaluation with methionine PET. *Radiology*. 1993;186(1):45–53.

27. Juhasz C, Chugani DC, Muzik O, et al. In vivo uptake and metabolism of alpha-[11C]methyl-L-tryptophan in human brain tumors. *J Cereb Blood Flow Metab*. 2006;26(3):345–357.
28. Kasper BS, Struffert T, Kasper EM, et al. 18Fluoroethyl-L-tyrosine-PET in long-term epilepsy associated glioneuronal tumors. *Epilepsia*. 2011;52(1):35–44.
29. Ishiwata K, Kubota K, Murakami M, et al. Re-evaluation of amino acid PET studies: can the protein synthesis rates in brain and tumor tissues be measured in vivo? *J Nucl Med*. 1993;34(11): 1936–1943.
30. Langen KJ, Ziemons K, Kiwit JC, et al. 3-[123I]Iodo-alpha-methyltyrosine and [methyl-11C]-L-methionine uptake in cerebral gliomas: a comparative study using SPECT and PET. *J Nucl Med*. 1997;38(4):517–522.
31. Langen KJ, Muhlensiepen H, Holschbach M, et al. Transport mechanisms of 3-[123I]Iodo-alpha-methyl-L-tyrosine in a human glioma cell line: comparison with [3H]methyl]-L-methionine. *J Nucl Med*. 2000;41(7):1250–1255.
32. Sato N, Suzuki M, Kuwata N, et al. Evaluation of the malignancy of glioma using 11C-methionine positron emission tomography and proliferating cell nuclear antigen staining. *Neurosurg Rev*. 1999; 22(4):210–214.
33. Roelcke U, Radu EW, von Ammon K, et al. Alteration of blood–brain barrier in human brain tumors: comparison of [18F]fluorodeoxyglucose, [11C]methionine and rubidium-82 using PET. *J Neurol Sci*. 1995; 132(1):20–27.
34. Prayson RA, Morris HH, Estes ML, et al. Dysembryoplastic neuroepithelial tumor: a clinicopathologic and immunohistochemical study of 11 tumors including MIB1 immunoreactivity. *Clin Neuropathol*. 1996; 15(1):47–53.
35. Miller DC, Lang FF, Epstein FJ. Central nervous system gangliogliomas. Part 1: pathology. *J Neurosurg*. 1993;79(6):859–866.
36. Prayson RA, Khajavi K, Comair YG. Cortical architectural abnormalities and MIB1 immunoreactivity in gangliogliomas: a study of 60 patients with intracranial tumors. *J Neuropathol Exp Neurol*. 1995;54(4):513–520.
37. Madakasira PV, Simkins R, Narayanan T, et al. Cortical dysplasia localized by [11C]methionine positron emission tomography: case report. *AJNR Am J Neuroradiol*. 2002;23(5):844–846.
38. Sasaki M, Kuwabara Y, Yoshida T, et al. Carbon-11-methionine PET in focal cortical dysplasia: a comparison with fluorine-18-FDG PET and technetium-99m-ECD SPECT. *J Nucl Med*. 1998;39(6):974–977.
39. Hammond RR, Duggal N, Woulfe JM, et al. Malignant transformation of a dysembryoplastic neuroepithelial tumor. Case report. *J Neurosurg*. 2000;92(4):722–725.